



# Minimizing position uncertainty for under-ice autonomous underwater vehicles <sup>☆</sup>



Baozhi Chen <sup>\*</sup>, Dario Pompili

*Department of Electrical and Computer Engineering, Rutgers University, New Brunswick, NJ, United States*

## ARTICLE INFO

### Article history:

Received 30 January 2013

Received in revised form 15 September 2013

Accepted 17 September 2013

Available online 25 September 2013

### Keywords:

Underwater acoustic sensor networks

Autonomous underwater vehicle

Localization

Position uncertainty

## ABSTRACT

Localization underwater has been known to be challenging due to the limited accessibility of the Global Positioning System (GPS) to obtain absolute positions. This becomes more severe in the under-ice environment since the ocean surface is covered with ice, making it more difficult to access GPS or to deploy localization infrastructure. In this paper, a novel solution that minimizes localization uncertainty and communication overhead of under-ice Autonomous Underwater Vehicles (AUVs) is proposed. Existing underwater localization solutions generally rely on reference nodes at ocean surface or on localization infrastructure to calculate positions, and they are not able to estimate the localization uncertainty, which may lead to the increase of localization error. In contrast, using the notion of external uncertainty (i.e., the position uncertainty as seen by others), our solution can characterize an AUV's position with a probability model. This model is further used to estimate the uncertainty associated with our proposed localization techniques. Based on this uncertainty estimate, we further propose algorithms to minimize localization uncertainty and communication overhead. Our solution is emulated and compared against existing solutions, showing improved performance.

© 2013 Elsevier B.V. All rights reserved.

## 1. Introduction

UnderWater Acoustic Sensor Networks (UW-ASNs) [2] consist of a number of sensors and vehicles that interact to collect data and perform tasks in a collaborative manner underwater. They have been deployed to carry out collaborative monitoring tasks including oceanographic data collection, climate monitoring, disaster prevention, and navigation. Autonomous Underwater Vehicles (AUVs) are widely believed to be revolutionizing oceanography and are enabling research in environments that have typically been impossible or difficult to reach. For example, AUVs have been used for continuous measurement of fresh

water exiting the Arctic through the Canadian Arctic Archipelago and Davis Strait in order to study the impact of climate change to the circulation of the world's oceans. The ability to do so under ice is important so that, for example, scientists can measure how much fresh water flows through the strait – and at what times of year – so they have a baseline for comparison in coming years.

For these missions, position information is of vital importance in mobile underwater sensor networks, as the data collected has to be associated with appropriate location in order to be spatially reconstructed onshore. Even though AUVs can surface periodically (e.g., every few hours) to locate themselves using Global Positioning System (GPS) – which does not work underwater – over time, inaccuracies in models for deriving position estimates, self-localization errors, and drifting due to ocean currents will significantly increase the uncertainty in position of underwater vehicle, which affects the performance of communication solutions such as [3]. Moreover, in

<sup>☆</sup> A preliminary shorter version of this article is in Proc. of IEEE Communications Society Conference on Sensor, Mesh and Ad Hoc Communications and Networks (SECON), June, 2012 [1].

<sup>\*</sup> Corresponding author. Tel.: +1 7324456400281.

E-mail addresses: [baozhi\\_chen@cac.rutgers.edu](mailto:baozhi_chen@cac.rutgers.edu) (B. Chen), [pompili@ece.rutgers.edu](mailto:pompili@ece.rutgers.edu) (D. Pompili).

extreme environments such as under ice, surfacing to get a GPS update is hardly possible and, therefore, position information is highly uncertain. In such environments, relying on standard navigation techniques such as Long Baseline (LBL) navigation is difficult as the use of static LBL beacons typically limits the operation range to about 10 km [4] and requires great deployment efforts before operation, especially in deep water (more than 100 m deep).

As AUVs are becoming more and more capable and also affordable, deployment of multiple AUVs to finish one mission becomes a widely-adopted option. This not only enables new types of missions through cooperation but also allows individual AUVs of the team to benefit from information obtained from other AUVs. Existing localization schemes underwater generally rely on the deployment of transponders or nodes with underwater communication capabilities as reference points, which requires either much deployment effort or much communication overhead (Note that in this work, reference nodes are the nodes whose positions are used by another node for localization). Moreover, these schemes are not able to estimate the uncertainty associated with the calculated position, which is high in under-ice environments, and thus are not able to minimize position uncertainty.

To address this problem, we propose a solution that uses only a subset of AUVs without relying on localization infrastructure. Specifically, a position uncertainty model in [5] is introduced to characterize an AUV's position. This model is extended to estimate the uncertainty associated with the standard distance-based localization technique, resulting in the distance-based localization with uncertainty estimate (DISLU). We further propose a Doppler-based technique with uncertainty estimation capability, which is called Doppler-based localization with uncertainty estimate (DOPLU). DISLU relies on packets (i.e., communication overhead) to measure the inter-vehicle distances (i.e., ranging), which, in conjunction with positions of reference nodes (in general *other AUVs*), are utilized to estimate the position. On the other hand, DOPLU, which measures Doppler shifts from ongoing communications and then uses these measurements to calculate velocities for localization, removes the need for ranging packets. As DOPLU only relies on relative measurements, it may not be able to fix displacement errors introduced by the rotation or position translation of the AUV group. In this case, DISLU is executed to bound such localization errors. Considering these tradeoffs, using the uncertainty model, the localization error and communication overhead of DISLU and DOPLU can be jointly considered and algorithms are devised to minimize the localization uncertainty and communication overhead while satisfying localization error requirement.

Our solution offers a way to estimate the degree of uncertainty associated with a localization technique and based on this estimation it further minimizes both position uncertainty and communication overhead. The contributions of this work include: (1) a probability model to estimate the position uncertainty associated with localization techniques; (2) an algorithm to minimize localization uncertainty by selecting an appropriate subset of reference

nodes; (3) an algorithm to optimize the localization interval in order to further minimize the localization overhead; and (4) a Doppler-based localization technique that can exploit ongoing communications for localization.

Compared to the previous shorter version [1], we added a section to discuss the relationship between these two notions and then presented applications and research areas where the proposed notion of external uncertainty can be applied to improve performance. Moreover, in the previous version, the internal uncertainty transmitted to the neighbor vehicle was directly used as the external uncertainty without considering the propagation of position uncertainty after delay and transmission loss of the uncertainty information. In this manuscript, we proposed a novel approach to estimate the external uncertainty based on the transmitted internal uncertainty. At last, more simulations are added to evaluate the accuracy of our proposed algorithms to estimate the external uncertainty.

The remainder of this paper is organized as follows. In Section 2, we review the related work for localization algorithms in UW-ASNs. We present the motivation and background in Section 3 and propose our solution in Section 4; in Section 5, performance evaluation and analysis are carried out, while conclusions are discussed in Section 6.

## 2. Related work

Localization is essential for underwater vehicle navigation and UW-ASNs, where many localization solutions, as summarized in [4,6], have been proposed. Due to space limitation, we just review the work that is most related, i.e., localization in UW-ASNs using AUVs.

Short Baseline (SBL) and Long Baseline (LBL) systems [4] are standard ways to localize vehicles underwater, where external transponder arrays are employed to aid localization. In SBL systems, position estimate is determined by measuring the vehicle's distance from three or more transponders that are, for example, lowered over the side of the surface vessel. LBL systems are similar to SBL, with the difference that an array of transponders is tethered on the ocean bed with fixed locations.

In [7], a localization scheme called AUV Aided Localization (AAL) is proposed, where position estimation is done using a single AUV. In AAL, an AUV navigates a predefined trajectory, broadcasts its position upon a node's request, and fixes its own position at the surface. Each node estimates the distances to the AUV while the AUV is at different locations, using the Round-Trip Time (RTT) between itself and the AUV. Algorithms such as triangulation or bounding box can then be used for position estimate. Another localization solution called Dive-N-Rise Localization (DNRL) is proposed for both static and mobile networks in [8]. DNRL is similar to AAL, with the difference that ocean currents are considered and time synchronization is required between nodes.

In [9], an online algorithm for cooperative localization of submerged AUVs is designed, implemented, and evaluated through experiments. This algorithm relies on a single surface vehicle called Communication and Navigation Aid (CNA) for autonomous navigation. Using the CNA's GPS

positions and basic onboard measurements including velocity, heading and depth, this algorithms can use filtering techniques such as Extended Kalman Filter (EKF) to bound the error and uncertainty of the on-board position estimates of a low-cost AUV.

Among existing underwater localization techniques (which are generally not suitable for under-ice environments), relatively few under-ice localization techniques have been proposed. Despite these efforts, the technology remains expensive and out of reach for researchers. Current techniques employed in the under-ice environment include combinations of either dead-reckoning using inertial measurements, sea-floor acoustic transponder networks such as SBL or LBL, and/or a Doppler Velocity Log (DVL) that can be either seafloor or ice relative [4]. These current approaches require external hardware, are cost prohibitive, and suffer from error propagation. For accurate dead reckoning, highly accurate sensors are required because magnetic navigation systems are subject to local magnetic field variations and gyros are subject to drift over time. Quality inertial navigation sensors often cost more than \$10,000 [4]. In contrast, our solution is much more economical as it does not require these expensive sensors.

Two solutions for underwater collaborative localization using a probability framework are proposed in [10,11], where a sum-product algorithm and a Markov process that are based on the so-called factor graph are used to model the joint distribution of multiple nodes. Both solutions require the global information of the nodes that are involved in localization, which leads to high computation complexity and communication overhead. Our solution offers another probability framework that leverages the self-estimated uncertainty distribution for estimation of other nodes. Therefore, global information is not required, resulting in reduced computation complexity and communication overhead.

### 3. Motivation and background

In UW-ASNs, inaccuracies in models for position estimation, self-localization errors, and drifting due to ocean currents will significantly increase the uncertainty in the position of an underwater vehicle. Hence, using a deterministic point is not enough to characterize the position of an AUV. Furthermore, such a deterministic approach underwater may lead to problems such as routing errors in inter-vehicle communications, vehicle collisions, loss of synchronization, mission failures. In order to address the problems due to position uncertainty, we introduce a probability model to characterize a node's position. In many applications such as geographic routing, AUVs need to estimate the positions of themselves and other AUVs'. Therefore, depending on the view of the different nodes, two forms of position uncertainty are defined, i.e., *internal* and *external uncertainty*. *Internal uncertainty* is the position uncertainty associated with a particular entity/node (such as an AUV) as seen by itself, while *external uncertainty* is the position uncertainty as seen by others, respectively.

These two notions introduce a shift in AUV localization: from a deterministic to a probabilistic view. This shift can

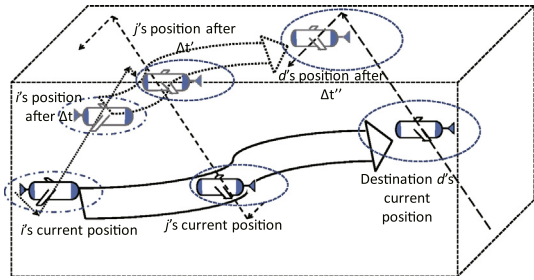
then be leveraged to improve the performance of solutions to problems in a variety of fields. Many approaches such as those using Kalman Filter (KF) [12] have been proposed to estimate the internal uncertainty assuming that the variables to be estimated have linear relationships between each other and that noise is additive and Gaussian. While simple and quite robust, KF is not optimal when the linearity assumption between variables does not hold. On the other hand, approaches using non-linear filters such as the extended or unscented KF attempt to minimize the mean squared errors in estimates by jointly considering the navigation location and the sensed states or features such as underwater terrain features, which are non-trivial, especially in an unstructured underwater environment.

Let us denote the internal uncertainty, a 3D region associated with any node  $j \in \mathcal{N}$  where  $\mathcal{N}$  is the set of network nodes, as  $\mathcal{U}_{jj}$ , and the external uncertainties, 3D regions associated with  $j$  as seen by  $i$ ,  $k \in \mathcal{N}$ , as  $\mathcal{U}_{ij}$  and  $\mathcal{U}_{kj}$ , respectively ( $i \neq j \neq k$ ). In general,  $\mathcal{U}_{ij}$ ,  $\mathcal{U}_{ij}$ , and  $\mathcal{U}_{kj}$  are different from each other; also, due to *information asymmetry*,  $\mathcal{U}_{ij}$  is in general different from  $\mathcal{U}_{ji}$ . External uncertainties may be derived from the broadcast/propagated internal-uncertainty estimates (e.g., using *one-hop* or *multi-hop neighbor discovery mechanisms*) and, hence, will be affected by end-to-end (e2e) *network latency* and *information loss*.

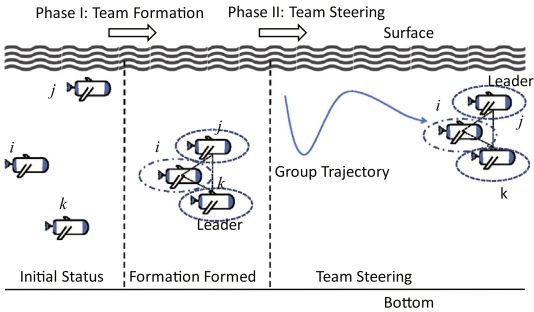
We present here applications and research areas where the proposed notion of external uncertainty can be applied to improve performance.

*Communication protocols for UW-ASNs:* In UW-ASNs, the external uncertainty can be used to improve the performance of networking solutions. For example, as shown in [5], a solution that considers external uncertainty can be used for Delay-Tolerant Networks (DTNs). As shown in Fig. 1(a) (where the single dotted arrow denotes the predictable trajectory and the double dotted arrow denotes the estimated data forwarding path), by leveraging the predictability of AUVs' trajectories, delaying packet transmissions in such a way as to wait for the optimal network topology (thus trading e2e delay for throughput and/or energy consumption) can minimize communication energy consumption for delay-tolerant traffic. Also, by optimizing statistically the transmission output power, routing errors can be reduced, which decreases energy/bandwidth utilization.

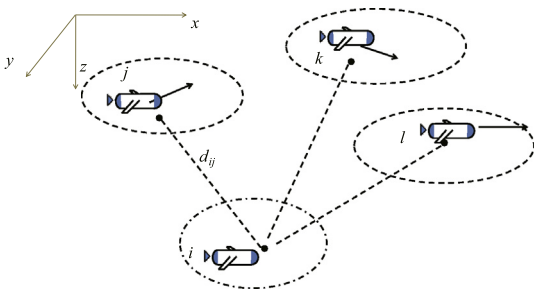
*Underwater robotics:* In underwater robotics, a team of AUVs can collaborate to explore a 3D region and take measurements in space and time. To derive the spatio-temporal correlation of the measurements, these AUVs need to keep a geometric formation and steer through the region (Fig. 1(b)). They also need to keep a distance between each other in order to avoid vehicle collisions. In [13], a solution is proposed to minimize the time to form the geometric formation while avoiding collisions. However, that solution assumes the gliders to have correct location information, which is a strong requirement in the underwater environment. The solution can be made more robust against ocean currents and acoustic channel impairments by exploiting the concept of external uncertainty, e.g., a control algorithm can be designed to minimize the probability that two AUVs are within the collision region. This concept can also be used to adapt the sampling strategy



(a) Energy minimization for DTNs



(b) Collision avoidance for team formation/steering



(c) Uncertainty minimization in localization

**Fig. 1.** Research areas that can benefit from the notion of external uncertainty (broken-line circles denote external uncertainty and broken-dotted-line circles denote internal uncertainty; note that we use circles instead of 3D shapes for uncertainty regions just for the sake of visualization simplicity).

based on the variation of the measurements. For example, for real-time ocean forecasting, a team of AUVs can be deployed to take spatial and temporal measurements. To maximize the forecasting performance, the geometry formation and inter-vehicle distance can be dynamically adjusted to measure a dynamically changing region. By using the external uncertainty notion, we can estimate the probability distribution of the measurements (since location of the measurement is the same as the AUV) and then design an optimal strategy to minimize the observation uncertainty for accurate forecasting.

*Underwater localization:* To perform self-localization, AUVs may need to rely on other anchor nodes (e.g., AUVs) whose positions may not be accurate (Fig. 1(c)). Localization errors, however, may increase if an AUV relies on anchors with large position uncertainty. The external-uncertainty notion can be used to decrease errors and

computation complexity, e.g., by selecting the optimal subset of anchors (with small external uncertainty) so to minimize its new internal uncertainty.

*Task allocation:* The proposed notion of uncertainty can also be applied in task allocation, whose objective is to choose a subset of vehicles to accomplish reliably a mission with specific requirements, e.g., only part of a team of AUVs can be selected to conduct a critical mission while trying to maximize the remaining energy after the mission or to minimize the time to complete the mission [14]. By using the external-uncertainty notion, a team of AUVs that are “closer” to the target can be selected, which may lead probabilistically to less time and/or energy to complete the mission.

*Data processing and visualization:* Once the measurements are received by the onshore station, oceanographers need to visualize and analyze sensor data for a multitude of ocean science studies. The external-uncertainty notion can improve the quality of 3D data reconstruction because it shows the vehicle deviation from the original mission path.

In this work, we illustrate that these two notions can be used to improve the performance in *underwater localization*.

#### 4. Proposed solution

With the notion of external uncertainty, we can model the uncertainty associated with localization techniques. Based on this uncertainty, optimization problems are formulated to minimize localization uncertainty and communication overhead. In this section, we first show how external uncertainty can be used to estimate the uncertainty with the standard distance-based localization technique (i.e., DISLU). Then we propose a novel Doppler-based localization technique DOPLU that jointly estimates localization uncertainty. DISLU requires ranging packets to measure the distances for position calculation, which introduces communication overhead. This weakness in DISLU can be offset by DOPLU, which exploits ongoing inter-vehicle communications to avoid the need for ranging packets. Such an ‘opportunistic’ approach (i.e., DOPLU) does not guarantee correct absolute locations (as Doppler shifts only characterize *relative* position change) so the team of AUVs needs to go back to DISLU to correct the locations when the error is too large. Based on this idea, we propose algorithms to solve two optimization problems, one for minimization of localization uncertainty and the other for minimization of communication overhead.

The communication protocol for our solution is presented in Fig. 2. Each AUV first runs DISLU using the distances measured from the round-trip time. Then, DOPLU is run using Doppler-shift information extracted from inter-vehicle packets. By overhearing the ongoing packets from the reference nodes, AUV *i* estimates the Doppler shifts and then extracts the relative velocity, from which the AUVs calculate their absolute velocities. DISLU is run to fix the localization error introduced by DOPLU after  $T_p$ , which is the time after the last DISLU is started ( $T_s$  is the duration for which enough Doppler shifts are collected to estimate the position).

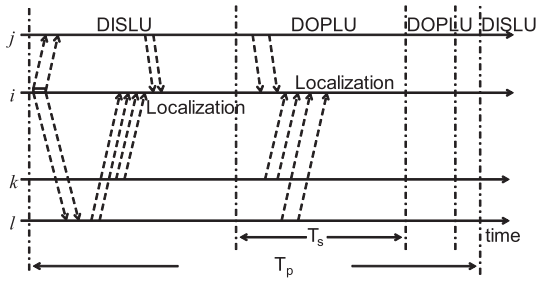


**Fig. 2.** Overview of the proposed approach (paired arrows represent the start and the end of one packet).

Both DISLU and DOPLU use the external uncertainty and corresponding probability distribution function (pdf) to estimate the uncertainty resulted from the localization technique, i.e., the internal uncertainty and pdf of the AUV running the localization algorithm. Then this internal uncertainty information is broadcast for other AUVs to estimate external uncertainties. Our previous work in [5] provided a *statistical solution* to estimate the internal uncertainty, while internal uncertainty is used as the external uncertainty (which is inaccurate).

In Section 4.1, we briefly review the formula to estimate internal uncertainty of underwater gliders, and then we propose an approach to estimate their external uncertainty. In Section 4.2, we present our DISLU algorithm, followed by the DOPLU algorithm in Section 4.3. In the end of this section, we further present an optimization algorithm to minimize the communication overhead.

4.1. Estimation of internal and external uncertainty

After receiving  $j$ 's internal uncertainty  $\mathcal{U}_{ji}$ , AUV  $i$  can update the estimate of  $j$ 's external uncertainty  $\mathcal{U}_{ij}$ . AUV  $j$ 's internal uncertainty can be estimated using statistical methods such as that presented in [5], where an underwater glider's internal uncertainty can be described by parameters  $(\bar{P}, \bar{t}, \bar{\mathbf{v}}, H_U, H_L, R)$ . Here we assume glider  $j$ 's estimated coordinates,  $P_n = (x_n, y_n, z_n)$  at sampling times  $t_n$  ( $n = 1, \dots, N$ ), as shown in [5], its trajectory segment can be described as  $P(t) = \bar{P} + \bar{\mathbf{v}}(t - \bar{t})$ , where  $\bar{P} = (\bar{x}, \bar{y}, \bar{z}) = \frac{1}{N} \sum_{n=1}^N (x_n, y_n, z_n)$  and

$$\bar{\mathbf{v}} = \frac{\|\overrightarrow{\bar{P}_1 P_N}\|}{\|(a^*, b^*, c^*)\| \cdot (t_N - t_1)} \cdot (a^*, b^*, c^*).$$

Here,  $[a^*, b^*, c^*]^T$  is the singular vector of  $N \times 3$  matrix

$$\mathbf{A} = [(x_1 - \bar{x}, \dots, x_N - \bar{x})^T, (y_1 - \bar{y}, \dots, y_N - \bar{y})^T, (z_1 - \bar{z}, \dots, z_N - \bar{z})^T]$$

corresponding to its largest absolute singular value,  $\bar{t} = \frac{1}{N} \sum_{n=1}^N t_n$  is the average of the sampling times, and  $\bar{P}_i$  is the projection of point  $P_i$  on the line segment. The internal-uncertainty region of  $j$  is estimated as a *cylindrical region* [5]  $\mathcal{U}_{ji}$  described by its radius  $R$  and its height  $H_U - H_L$ , where  $H_U$  and  $H_L$  - in general different - are the *signed distances* of the cylinder's top and bottom surface (i.e., the surface ahead and behind in the trajectory direction, respectively) to glider  $j$ 's expected location on

the trajectory.  $H_U, H_L$  and  $R$  can be calculated using  $P_n$  ( $n = 1, \dots, N$ ) (see [5] for more details).

Due to packet delays and losses in the network,  $j$ 's external-uncertainty regions as seen by single- and multi-hop neighbors are *delayed versions* of  $j$ 's own internal uncertainty. Hence, when using *multi-hop neighbor discovery schemes*, the internal uncertainty  $\mathcal{U}_{ij}$  provides a *lower bound* for all the external uncertainties associated with that node,  $\mathcal{U}_{ij}, \forall i \in \mathcal{N}$ . Consequently, we derive  $\mathcal{U}_{ij}$  based on the received  $\mathcal{U}_{ji}$ .

We use Unscented Kalman Filter (UKF) to predict how the internal uncertainty 'propagates' through the network. This is done in two steps detailed below: (1) *Region Prediction* - this is to predict the current position of an AUV assuming that its previous location is at a point in the internal-uncertainty region; then, the external-uncertainty region is obtained by taking the set containing these predicted positions; and (2) *Distribution Estimation* - this is to calculate the probability density function (pdf) of the current position by integrating the internal-uncertainty pdf over points with the same predicted position.

(1) *Region Prediction*: AUV  $i$  first needs to predict  $j$ 's position assuming  $j$  is located at a point in  $\mathcal{U}_{ji}$  and then considers the union of these predicted points. The movement model of  $j$  can be described using the following nonlinear dynamical system. The equivalent discrete-time dynamic equation can be derived as in [15] by means of the state-space method using iterations. AUV  $i$  estimates the state from step  $q = 1$  whenever  $\mathcal{U}_{ij}$  is received and  $q$  is incremented until a new  $\mathcal{U}_{ij}$  is received ( $q$  is reset to 1 upon receiving this information). Hence,

$$\mathbf{s}_j^q = \mathbf{F}_j \mathbf{s}_j^{q-1} + \mathbf{o}(\mathbf{s}_j^{q-1}) + \mathbf{G} \mathbf{u}_j^{q-1} + \mathbf{B} \mathbf{w}_j^{q-1} \tag{1}$$

represents the state-transition equation for the system describing the motion of AUV  $j$  between steps  $q - 1$  and  $q$ . In this equation,

$$\mathbf{s}_j^q = [x_j^q, y_j^q, z_j^q, \dot{x}_j^q, \dot{y}_j^q, \dot{z}_j^q, v_{j,x}^{oc}, v_{j,y}^{oc}, v_{j,z}^{oc}]^T$$

represents 3D position  $(x_j^q, y_j^q, z_j^q)$ , velocity  $(\dot{x}_j^q, \dot{y}_j^q, \dot{z}_j^q)$ , and ocean-current velocity  $(v_{j,x}^{oc}, v_{j,y}^{oc}, v_{j,z}^{oc})$  of AUV  $j$  at step  $q$ .  $\mathbf{o}(\mathbf{s}_j^{q-1})$  is the ocean-current prediction function (which is generally nonlinear),  $\mathbf{u}_j^{q-1} = [u_j^{q-1,x}, u_j^{q-1,y}, u_j^{q-1,z}]^T$  is the control input (such as position displacement due to acceleration and turning driven by propeller) for  $t \in [(q - 1)T, qT)$ , and  $\mathbf{w}_j^{q-1} = [w_j^{q-1,x}, w_j^{q-1,y}, w_j^{q-1,z}, w_{oc,j}^{q-1,x}, w_{oc,j}^{q-1,y}, w_{oc,j}^{q-1,z}]^T$  represents discrete random acceleration caused by non-ideal noise in the control input and/or the variation in ocean current speed. Note that  $\mathbf{o}(\mathbf{s}_j^{q-1})$  can be predicted using ocean-current models or data from real-time on-shore ocean observing systems; also, AUVs are spaced apart so currents affecting different AUVs are generally different.

In (1),  $\mathbf{F}_j, \mathbf{G}$ , and  $\mathbf{B}$  are matrices to adjust the state  $\mathbf{s}_j^q$  according to the previous state, control input, and random acceleration noise, respectively, and are defined as

$$\mathbf{F}_j = \begin{bmatrix} \mathbf{I}_3 & T'_j \mathbf{I}_3 & T'_j \mathbf{I}_3 \\ 0 & \mathbf{I}_3 & 0 \\ 0 & 0 & 0 \end{bmatrix}, \quad \mathbf{G} = \begin{bmatrix} 0 \\ \mathbf{I}_3 \\ 0 \end{bmatrix}, \quad \mathbf{B} = \begin{bmatrix} 0 & 0 \\ \mathbf{I}_3 & 0 \\ 0 & \mathbf{I}_3 \end{bmatrix},$$

where  $\mathbf{I}_3$  is the  $3 \times 3$  identity matrix,  $T'_j$  is the difference between the current time and the last time when  $\mathcal{U}_{ij}$  was estimated or the last update time that UKF was run, i.e.,  $T'_j = t_{\text{now}} - t_{\mathcal{U}_{ij}}$  if  $i$  receives  $j$ 's updated internal uncertainty after the last UKF update, whereas  $T'_j = T$  if  $i$  does not receive  $j$ 's update message, where  $t_{\mathcal{U}_{ij}}$  is the time when  $\mathcal{U}_{ij}$  is estimated by  $j$  and  $T$  is the UKF update interval. Note that, when used as superscript,  $T$  indicates matrix transpose; otherwise, it represents the time interval.

The variable  $\mathbf{w}_j^{q-1}$  represents 3D samples of discrete time white Gaussian noise; hence,  $\mathbf{w}_j^{q-1} \sim \mathcal{N}(0, \mathbf{Q})$ , where  $\mathbf{Q} \geq 0$  is the covariance matrix of the process. The random acceleration is also assumed to be independent on the three axes. Here we assume that an AUV can measure the ocean-current velocity using sensors such as Acoustic Doppler Current Profiler (ADCP), which are, however, expensive; for AUVs without ADCP, we can force the state for ocean current to be zero, where the model reduces to a linear KF and the effect of ocean current should be treated as noise in  $\mathbf{w}_j^q$ .

Using (1), AUV  $j$ 's external uncertainty can then be estimated using Unscented Kalman Filter [16]. That is, by taking one point in  $\mathcal{U}_{ij}$  as  $j$ 's original position to calculate  $j$ 's current position, and then take the union of all the calculated positions, which is the current external uncertainty.

(2) *Distribution Estimation*: Let  $\mathbf{p} \in \mathcal{U}_{ij}^q$ , assume  $\mathbf{p}$  is predicted from point  $\mathbf{p}'$  at step  $q-1$ , i.e.,  $\mathbf{p} = h_{\text{UKF}}(qT, \mathbf{p}', (q-1)T)$ ,  $\mathbf{p}' \in \mathcal{U}_{ij}^{q-1}$ . The pdf  $g_{ij}^q(\mathbf{p})$  of the external uncertainty  $\mathcal{U}_{ij}^q$  at step  $q$  can be derived from the pdf  $g_{ij}^{q-1}(\mathbf{p})$  of  $\mathcal{U}_{ij}^{q-1}$  as

$$g_{ij}^q(\mathbf{p}) = \int g_{ij}(\mathbf{p} = h_{\text{UKF}}(qT, \mathbf{p}', (q-1)T) | \mathbf{p}' \in \mathcal{U}_{ij}^{q-1}) g_{ij}^{q-1}(\mathbf{p}') d\mathbf{p}'.$$

Here  $g_{ij}(\mathbf{p} = h_{\text{UKF}}(qT, \mathbf{p}', (q-1)T) | \mathbf{p}' \in \mathcal{U}_{ij}^{q-1})$  is the conditional pdf, i.e., given the position  $\mathbf{p}'$  at time  $(q-1)T$ , the pdf of  $\mathbf{p}$  at time  $qT$ ; and  $g_{ij}^{q-1}(\mathbf{p}')$  is the pdf of the AUV position at time  $(q-1)T$ .

With the help of UKF and the probability theory, we can derive the external uncertainty and its pdf. Note that the initial pdf  $g_{ij}^0(\mathbf{p})$  is the  $t$ -distribution on  $\mathcal{U}_{ij}$  (i.e.,  $\mathcal{U}_{ij}^0$ ) received from  $j$ . To reduce the complexity, we convert an uncertainty region (internal or external) into its discrete counterparts, i.e., we divide an uncertainty region into a finite number of equal-size small regions. When the number of small regions is sufficiently large, the UKF filtering on each small region can be approximated by the UKF filtering on a point – e.g., the *centroid* – in this small region. Hence, the predicted external-uncertainty region can be approximated as the region contained in the hull of these predicted points. The pdf functions are also approximated by the probability mass functions on discrete points, which simplifies the pdf estimation after UKF filtering.

#### 4.2. Distance-based Localization with Uncertainty Estimate (DISLU)

We present here the DISLU technique, which is based on the following idea: to estimate its own position, vehicle  $i$  needs (1) to *estimate the distances* between itself and its reference vehicles, and (2) to *estimate its own position* based on these distances.

DISLU relies on the round-trip time  $T_{RTT}$  to measure the inter-vehicle distance. By extracting the one-way propagation time,  $i$  is able to calculate the inter-vehicle distance. That is, the distance between transmitter  $i$  and receiver  $j$  is

$$d_{ij} = c \cdot \left( T_{RTT} - T_i^{(TX)} - T_j^{(TX)} - T_j^{(hold)} \right) / 2,$$

where  $T_i^{(TX)}$  and  $T_j^{(TX)}$  are the duration to transmit the packet at  $i$  and the duration to transmit acknowledgement at  $j$  (i.e., transmission delays),  $T_j^{(hold)}$  is the holdoff time of  $j$  to avoid collisions. To reduce the transmission time, we can use the short ping packets (e.g., the mini-packet provided by WHOI modem). Once  $j$  receives the ping packet, it starts a hold-off timer,  $T_j^{(hold)}$ , which is a uniformly distributed random variable in  $[0, 2T_{hold}^{mean}]$  where  $T_{hold}^{mean}$  is given by,

$$T_{hold}^{mean} = \left( 1 - \frac{d_{ij}}{R} \right) \tau + \frac{\phi_{ij}}{c}, \quad (2)$$

where  $d_{ij}$  is the distance from  $i$  to  $j$ ,  $\tau$  is the estimated transmission time for the current packet,  $c = 1500$  m/s is the propagation speed of acoustic waves,  $R$  is the transmission radius of the underwater modem, and  $\phi_{ij} = \max\{0, R - d_{ij}\}$ . The first term in (2) gives less time to the neighbor that is closer to  $i$ , and the second term is the extra delay that a node should wait so that all the nodes receive the packet. This gives fairness by providing synchronization in starting the hold-off timers of all the nodes receiving the data packet.  $T_j^{(hold)}$  is then embedded in the acknowledge packet for  $i$ 's information.

After the calculation of  $d_{ij}$ 's,  $i$  estimates its own position as the point with the least mean squared error to the reference nodes. Then,  $i$  estimates its internal uncertainty region using *conditional probability* and the distribution of the reference nodes within their external-uncertainty regions.

Given the set of  $i$ 's neighbors  $\mathcal{N}_i$ , the external uncertainty regions  $\mathcal{U}_{ij}$ , the distances  $d_{ij}$ , and the pdf of  $j$  within region  $\mathcal{U}_{ij}$ ,  $\forall j \in \mathcal{N}_i$ ,  $i$  can estimate the pdf of being at generic point  $p$  as

$$\begin{aligned} g(P_i = p) &= \int_{p_j \in \mathcal{U}_{ij}, j \in \mathcal{N}_i} g \left( P_i = p, \bigcap_{j \in \mathcal{N}_i} P_j = p_j \right) \\ &= \int_{p_j \in \mathcal{U}_{ij}, j \in \mathcal{N}_i} \left[ g(P_i = p | \bigcap_{j \in \mathcal{N}_i} P_j = p_j) \cdot g \left( \bigcap_{j \in \mathcal{N}_i} P_j = p_j \right) \right]. \end{aligned} \quad (3)$$

Here  $g(P_i = p)$  is the pdf of the position of  $i$  at point  $p$ ,  $g(\cdot)$  denotes conditional probability density function (conditional pdf). In our solution,  $p$  is calculated as the point that has the minimum squared error, i.e.,  $p \in S_i$ , where  $S_i \equiv \{q = \arg \min \sum_{j \in \mathcal{N}_i} \|d(p, p_j) - d_{ij}\|^2\}$  (that is,  $\mathcal{U}_{ii} = S_i$ ). Here,  $d(p, p_j)$  is the distance between point  $p$  and  $p_j$ . Note

that  $S_i$  may have more than one element due to the Euclidean norm (e.g., there are two possible positions for the case with three reference nodes and corresponding distances to them known). Due to the symmetry in Euclidean space, we have

$$g\left(P_i = p \mid \bigcap_{j \in \mathcal{N}_i} P_j = p_j\right) = \begin{cases} 1/|S_i| & p \in S_i \\ 0 & p \notin S_i \end{cases}, \quad (4)$$

where  $|S_i|$  is the number of elements in  $S_i$  if  $S_i$  is a discrete set, or the area (or volume) of  $S_i$  if  $S_i$  is a non-empty non-discrete set (e.g., the case with two references).

The joint pdf,  $g(\bigcap_{j \in \mathcal{N}_i} P_j = p_j)$ , can be approximated as,

$$g\left(\bigcap_{j \in \mathcal{N}_i} P_j = p_j\right) \approx \prod_{j \in \mathcal{N}_j} g(P_j = p_j), \quad (5)$$

as the distributions of these AUVs are approximately independent. Since  $T_p$  and  $T_s$  are generally large (see Section 4.4), the positions of AUVs can be treated as independent after drifting for a long time (while accuracy derivation of the joint pdf is rather difficult). Therefore, (3) can be expanded as,

$$g(P_i = p) \approx \int_{p_j \in \mathcal{U}_{ij}, j \in \mathcal{N}_i} \left[ g\left(P_i = p \mid \bigcap_{j \in \mathcal{N}_i} P_j = p_j\right) \cdot \prod_{j \in \mathcal{N}_j} g(P_j = p_j) \right]. \quad (6)$$

Hence  $i$ 's internal uncertainty  $\mathcal{U}_{ii}$  with  $g(\cdot)$  being the pdf is estimated, which is then broadcast to other AUVs. AUVs receiving this information then use  $\mathcal{U}_{ii}$  to estimate  $i$ 's external uncertainty.

### 4.3. Doppler-based Localization with Uncertainty Estimate (DOPLU)

DOPLU runs between two consecutive run of DISLU. Since the vehicle location has 3 parameters to be determined, in general when the Doppler shifts from more than 3 nodes are extracted, an equation group can be formulated and DOPLU can be run. The time between two consecutive runs of the DISLU is divided into sub-slots with appropriate duration  $T_s$  (Fig. 2) so that the DOPLU will be run at an appropriate frequency. Within each sub-slot, the vehicle that runs DOPLU extracts Doppler shifts from the packet it overhears (even if the packet is not intended to be received by it) from the reference vehicles. With the additional information it obtains from the packet header (such as velocity of the reference node), it computes its own absolute velocity, which is then used to estimate its own position and internal uncertainty. This reduces the communication overhead for sending packets to estimate inter-vehicle distance.

An algorithm is designed so that  $T_s$  can be adjusted dynamically according to the frequency of ongoing communication activities. Within  $T_s$ , an AUV is expected to collect enough Doppler shifts from its reference neighbors so that the DOPLU algorithm runs efficiently. Note

that if  $T_s$  is too small, it is very likely that the velocity calculated by DOPLU is close to that obtained from the last calculation, which means waste of computation resources. On the other hand,  $T_s$  should not be too large as it would lead to too much localization error. The longer  $T_s$  is, the less frequent a AUV calculates its position to correct its velocity or position estimation error; this increases the error in position estimation.

In the rest of this section, we focus on the main problem, i.e., how to estimate the position and internal uncertainty when Doppler shifts are available, and leave the optimization of  $T_s$  in Section 4.4. Using the Doppler shifts regarding to the reference nodes,  $i$  can estimate its own absolute velocity using the projected positions (i.e., by adding past velocity times the time passed to past position) and velocities. Using this relationship for all reference nodes,  $i$  obtains an equation group to solve, where absolute velocity  $\vec{v}_i$  can be estimated.

To see how to calculate the absolute velocity, assume that at the end of one sub-slot, AUV  $i$  has collected the Doppler shift  $\Delta f_{ij}$  from reference node  $j$ . From the definition of Doppler shift, we have  $\Delta f_{ij} = -\frac{\vec{v}_{ij} \circ \vec{P}_i \vec{P}_j}{\|P_i P_j\|} \frac{f_0}{c}$ , where  $\vec{v}_{ij}$  is the

relative velocity of  $i$  to  $j$ ,  $\vec{P}_i \vec{P}_j$  is the position vector from  $i$  to  $j$ ,  $f_0$  is the carrier frequency,  $c = 1500$  m/s is the speed of sound, and  $\circ$  is the inner product operation. From this equation, we have

$$\frac{\vec{v}_{ij} \circ \vec{P}_i \vec{P}_j}{\|P_i P_j\|} = -\Delta f_{ij} \frac{c}{f_0}. \quad (7)$$

Note that we assume the Doppler shift is estimated accurately. In reality, the frequency-dependent Doppler frequency spread is usually significant due to the inherently wideband nature of the underwater acoustic channel with low Q-factor. Moreover, the temporary variations in factors such as temperature, salinity, depth and ocean surface affect the acoustic speed and propagation path, while drifting due to ocean currents affects the motion of the transmitter and the receiver. All these lead to randomness in the Doppler measurements. Therefore, estimation of Doppler shifts is non-trivial and some solutions such as [17,18] have been proposed. To apply DOPLU, special design such as OFDM communication [19] can be applied in physical layer to deal with the generated inter-symbol interference. In this paper, we focus on the localization solution itself and assume the Doppler shift reading from acoustic modem – where appropriate Doppler estimation techniques have been applied – is accurate. Consideration of the randomness in Doppler reading in DOPLU is left as future work.

From (7), assume that  $i$  has collected the Doppler shifts of  $N_i^{(ref)}$  reference nodes, we then have an equation group with  $N_i^{(ref)}$  equations. We then can derive  $i$ 's velocity  $\vec{v}_i$ .

Assume  $\vec{v}_i = (v_x^{(i)}, v_y^{(i)}, v_z^{(i)})$  and  $\frac{\vec{P}_i \vec{P}_j}{\|P_i P_j\|} = (\alpha_x^{(ij)}, \alpha_y^{(ij)}, \alpha_z^{(ij)})$ , (7) is then

$$\begin{aligned}\vec{\mathbf{v}}_{ij} \circ \frac{\vec{P}_i \vec{P}_j}{\|\vec{P}_i \vec{P}_j\|} &= (\vec{\mathbf{v}}_i - \vec{\mathbf{v}}_j) \circ \frac{\vec{P}_i \vec{P}_j}{\|\vec{P}_i \vec{P}_j\|} \\ &= (v_x^{(i)} - v_x^{(j)})\alpha_x^{(ij)} + (v_y^{(i)} - v_y^{(j)})\alpha_y^{(ij)} \\ &\quad + (v_z^{(i)} - v_z^{(j)})\alpha_z^{(ij)} \\ &= -\Delta f_{ij} \frac{c}{f_0}.\end{aligned}$$

By manipulating this equation, we have

$$\begin{aligned}v_x^{(i)}\alpha_x^{(ij)} + v_y^{(i)}\alpha_y^{(ij)} &= -\Delta f_{ij} \frac{c}{f_0} - v_z^{(i)}\alpha_z^{(ij)} + v_x^{(j)}\alpha_x^{(ij)} + v_y^{(j)}\alpha_y^{(ij)} \\ &\quad + v_z^{(j)}\alpha_z^{(ij)}.\end{aligned}\quad (8)$$

In this equation,  $v_x^{(i)}$  and  $v_y^{(i)}$  in the left-hand side are variables to be solved, whereas  $v_z^{(i)}$  in the right-hand side can be derived from pressure sensor reading,  $(\alpha_x^{(ij)}, \alpha_y^{(ij)}, \alpha_z^{(ij)})$  is the normalized vector of  $\vec{P}_i \vec{P}_j$ , and  $(v_x^{(j)}, v_y^{(j)}, v_z^{(j)})$  is obtained from the velocity information embedded in the overheard packet header of  $j$ .

Considering all the  $N_i^{(ref)}$  reference nodes, we can obtain a linear equation group, which can be expressed in a matrix form as  $\mathbf{Ax} = \mathbf{b}$ , where

$$\mathbf{A} = \begin{bmatrix} \alpha_x^{i1} & \alpha_y^{i1} \\ \alpha_x^{i2} & \alpha_y^{i2} \\ \vdots & \vdots \\ \alpha_x^{iN_i^{(ref)}} & \alpha_y^{iN_i^{(ref)}} \end{bmatrix}, \quad \mathbf{x} = \begin{bmatrix} v_x \\ v_y \end{bmatrix}, \quad \mathbf{b} = \begin{bmatrix} b_{i1} \\ b_{i2} \\ \vdots \\ b_{iN_i^{(ref)}} \end{bmatrix}.\quad (9)$$

Here  $b_{ij} = -\Delta f_{ij} \frac{c}{f_0} - v_z^{(i)}\alpha_z^{(ij)} + v_x^{(j)}\alpha_x^{(ij)} + v_y^{(j)}\alpha_y^{(ij)} + v_z^{(j)}\alpha_z^{(ij)}$ . We want to find the optimal  $\mathbf{x}^*$  such that the sum of squared errors is minimized. That is,

$$\mathbf{x}^* = \arg \min \|\mathbf{b} - \mathbf{Ax}\|^2.\quad (10)$$

From *matrix theory*,  $\mathbf{x}^*$  can be solved as  $\mathbf{x}^* = (\mathbf{A}^T \mathbf{A})^{-1} \mathbf{A}^T \mathbf{b}$ . Once the velocity is calculated, the position of  $i$  is updated as  $p_i = p_i + \vec{\mathbf{v}} \cdot T_s$ , where  $\vec{\mathbf{v}} = [v_x^{(i)}, v_y^{(i)}, v_z^{(i)}]^T$ .

Assume that the uncertainty regions  $\mathcal{U}_{ij}$  and the distribution pdf of  $j$  within region  $\mathcal{U}_{ij}$  are known (by embedding these parameters in the header of the packet),  $\forall j \in \mathcal{N}_i$ ,  $i$  can estimate the pdf of being at point  $p$  as

$$\begin{aligned}g(P_i = p) &\approx \int_{p_j \in \mathcal{U}_{ij}, \forall j \in \mathcal{N}_i} \left[ g\left(P_i = p \mid \bigcap_{j \in \mathcal{N}_i} P_j = p_j\right) \cdot g\left(\bigcap_{j \in \mathcal{N}_i} P_j = p_j\right) \right].\end{aligned}$$

Similar to the case of DISLU,  $i$  can calculate the distribution of its own location and, hence, its internal uncertainty region.

**Minimization of Location Uncertainty:** Obviously, localization using different references leads to different estimation of internal uncertainty and corresponding pdf. Our objective is to minimize the estimated internal uncertainty. Using our notions of internal and external uncertainty, this can be achieved by solving an optimization problem. To measure the degree of uncertainty, we use *information entropy* as the metric, i.e.,

$$H(\mathcal{U}_{ij}, g_{ij}) = - \int_{p \in \mathcal{U}_{ij}} g_{ij}(p) \log(g_{ij}(p)) dp.\quad (11)$$

The bigger  $H(\mathcal{U}_{ij}, g_{ij})$  is, the more uncertain  $\mathcal{U}_{ij}$  is. The reason to use information entropy instead of simply the size of uncertainty region is that it can better characterize uncertainty. **Example:** Assume that an AUV's position is distributed in  $[0, 10]$  along  $x$ -axis (i.e., distributed on a line segment in the 3D space) with pdf being 9.9 in  $[0, 0.1]$  and  $0.1/99$  in  $[0.1, 10]$  (Case 1). Then its entropy is  $-3.17$  bits, which is less than the entropy 3.32 bits when the AUV is uniformly distributed in  $[0, 10]$  (Case 2) or the entropy is 3 bits when the AUV is uniformly distributed in  $[0, 8]$  (Case 3). Obviously Case 1 is the most certain in these 3 cases even though Case 2 has the same size and Case 3 has the smallest size of the region. Note that the information flow between AUVs can occur in loops; this may not amplify errors of the positioning algorithm, as our problem selects the neighbors that can minimize the uncertainty.

With this metric, the problem to minimize localization uncertainty can be formulated as,

**Given :**  $\mathcal{N}_i, \mathcal{U}_{ij}, g_{ij}()$ ;

**Find :**  $\mathcal{A}_i$ ; **Minimize :**  $H(\mathcal{U}_i, g_i)$ ;

$$\mathbf{S.t.} : \mathcal{U}_i \equiv \{q = \arg \min \sum_{j \in \mathcal{A}_i} \|d(p, p_j) - d_j\|^2\};\quad (12)$$

$$g(P_i = p) = \int_{p_j \in \mathcal{U}_{ij}, j \in \mathcal{A}_i} \left[ g\left(P_i = p \mid \bigcap_{j \in \mathcal{N}_i} P_j = p_j\right) \cdot \prod_{j \in \mathcal{A}_i} g(P_j = p_j) \right];\quad (13)$$

$$|\mathcal{A}_i| \geq 3; \quad \mathcal{A}_i \subset \mathcal{N}_i.\quad (14)$$

Here  $\mathcal{A}_i$  represents a subset of  $i$ 's reference nodes, (12) and (13) estimate the internal uncertainty and corresponding pdf when nodes in  $\mathcal{A}_i$  are used as references; and (14) are the constraints for  $\mathcal{A}_i$  so that enough reference nodes are selected for localization.

To reduce the complexity, we can convert an uncertainty region (internal or external) into discrete counterparts. That is, we divide an uncertainty region into a finite number of equal-size small regions. When the number  $K_i$  of small regions is sufficiently large, the pdf of the AUV's position on a point – such as the centroid – in this small region can therefore be approximated by the probability on a small region. Hence the estimated external-uncertainty region can be approximated as the region contained in the hull of these estimated points. The pdf functions are also be approximated by the probability mass functions on discrete points, which simplifies the pdf estimation. The above optimization can then be solved using exhaustive search algorithm after the discretization. The computation complexity of the exhaustive search is  $\mathcal{O}(2^{|\mathcal{A}_i|} K_i^{|\mathcal{A}_i|})$ . Since the number of AUVs is generally small, this complexity is mainly decided by  $K_i$ . Depending on the computation capability of the onboard processor, appropriate  $K_i$  can be used. Further improvement of the solution can be done after converting it into appropriate optimization that can be solved efficiently and we leave this as future work.

#### 4.4. Minimization of communication overhead

In this section, we discuss how to optimize  $T_s$  and  $T_p$  so that localization overhead can be minimized while keeping

the localization uncertainty low. We first propose an algorithm to dynamically adjust  $T_s$  in order to maintain the performance of DOPLU. Then,  $T_p$  is optimized to minimize the localization overhead.

As for  $T_s$ , it should be large enough so that packets from enough reference nodes are overheard. Suppose  $K_{\min}$  is the minimum number of reference nodes (or  $|\mathcal{A}_i|$  if the optimization algorithm in Section 4.3 is used) so that  $\mathbf{x}^*$  can be calculated using DOPLU. In the beginning,  $T_s$  is initialized as  $T_s = \frac{R}{c} + T_{TX} \cdot K_{\min}$ , i.e., the minimum time to overhear packets from  $K_{\min}$  reference nodes. Suppose that during the last  $T'_s$  period, Doppler shifts from  $N'$  reference nodes with smaller degree of uncertainty (seen by  $i$ ) than  $i$ 's are received. On average, it takes  $T'_s/N'$  to receive a useful Doppler shift. Then, the expected time to receive  $K_{\min}$  useful Doppler shifts is  $T'_s \cdot K_{\min}/N'$ . We update  $T_s$  using a weighted average. That is,  $T_s = \beta \cdot T'_s + (1 - \beta) \cdot T_s \cdot K_{\min}/N'$ , where  $\beta \in (0, 1)$  is a weight factor.

Using internal and external uncertainty, we can also optimize the interval  $T_p$  running DISLU. By optimizing  $T_p$ , we minimize the overhead to use DISLU and hence the overall overhead. DISLU is run when the localization error is large. The localization error can be estimated by calculating the distance from the position estimated by DISLU to that estimated by DOPLU. When the localization error is greater than a threshold  $d_{th}$ , DISLU is run to correct the error. Since the position is not deterministic, this requirement is expressed in a probabilistic way. That is, DISLU should be run when the probability of the localization error being over  $d_{th}$  is above a threshold probability  $\gamma$ . Therefore, to minimize the overhead of running DISLU,  $T_p$  should be maximal under the constraint that the probability of the localization error being over  $d_{th}$  is below  $\gamma$ . This can be formulated into the following optimization problem,

**Given :**  $\mathcal{U}_{ij}, \mathbf{g}_{ij}(), \gamma;$

**Find :**  $T_p^*; \quad \mathbf{Maximize} : T_p;$

**S.t. :**  $\Pr\{\|\tilde{p}_i(T_p) - \bar{p}_i(T_p)\| > d_{th}\} < \gamma,$

where  $\bar{p}_i(T_p)$  and  $\tilde{p}_i(T_p)$  are the prediction positions using the DOPLU and DISLU after  $T_p$  from the last DISLU run time,

respectively. This prediction of future internal uncertainty is based on the current estimated internal uncertainty and AUV's trajectory. A solution has been proposed in [5] for underwater gliders (one type of buoyancy-driven AUVs), which we adopt in this work. As the previous optimization problem, we can also convert it into discrete variable optimization problem and solve it in a similar way. Depending on the prediction method and the type of AUVs, the computation complexity varies. For example, using the prediction method in [5], the computation complexity is  $\mathcal{O}(K_i N_{smp})$  for underwater gliders with  $N_{smp}$  of position samples. Note that  $T_s$  and  $T_p$  can be jointly optimized, which is more complicated and hence is left as future work.

## 5. Performance evaluation

The communication solution is implemented and tested on our underwater communication emulator [20]. This emulator is composed of four WHOI Micro-Modems and a real-time audio processing card to emulate underwater channel propagation. The multi-input multi-output audio interface can process real-time signals to adjust the acoustic signal gains, to introduce propagation delay, to mix the interfering signals, and to add ambient/man-made noise and interference. Our solution is compared against AAL, DNRL, and CNA, as introduced in Section 2, under an environment that is described by the Bellhop model [21]. We use the typical Arctic sound speed profile as in [22] and the corresponding Bellhop profile is plotted in Fig. 3. Note that we use 25 kHz, the sound frequency in use for our WHOI modem. We modify AAL, DNRL, and CNA, as they were originally designed for settings that are quite different from the under-ice environment. Specifically, AAL, DNRL and CNA all use the AUV that surfaces last as reference node because intuitively the shorter an AUV stays underwater (the less time it stays in an uncertain environment after a GPS fix), the less uncertain its position is. Triangulation is employed for position calculation in AAL and DNRL, while EKF filtering is used in CNA. We are also interested in seeing the performance improvement that we get using the external uncertainty notion.

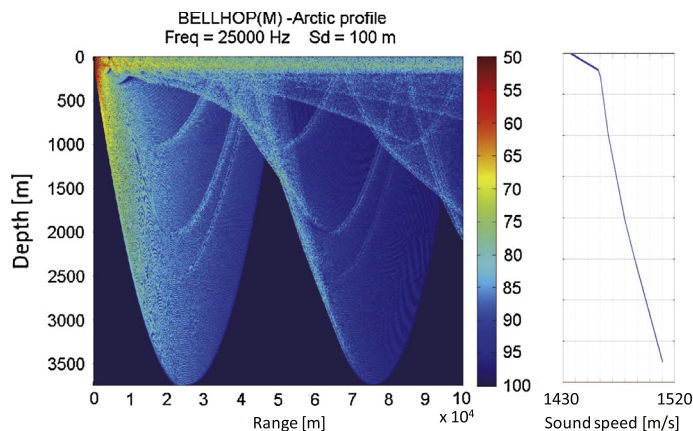


Fig. 3. Bellhop profile for typical Arctic environment.

**Table 1**

Simulation parameters.

|                                |  |
|--------------------------------|--|
| Total time                     | 10600 s (~2.94 h)  |
| Time interval, $\Delta T$      | 60 s   |
| Deployment 3D Region           | 2000(L) $\times$ 2000(W) $\times$ 1000(H) m <sup>3</sup> |
| Confidence parameter, $\alpha$ | 0.05   |
| AUV velocity                   | 0.25–0.40 m/s [23]                                       |
| AUV depth range                | [0, 1000] m [23]   |
| Typical currents               | 0.01–0.03 m/s [24]                                       |
| Extreme currents               | 0.04–0.06 m/s [24]                                       |
| Water temperature range        | [–2, 2] °C [25]  |
| Salinity range                 | [32.5, 35] ppt [23]                                      |

Therefore, we implement another version of our proposed solution without using external uncertainty, i.e., forcing the position uncertainty to be zero. We denote this modified version and the original version by ‘Proposed solution w/o EU’ and ‘Proposed solution w/ EU’, respectively.

In order to evaluate the localization performance, two metrics, the *localization error* and the *deviation of error*, are used. Localization error is defined as the distance between the actual and the estimated AUV position. The deviation of error is the amount the localization error deviating from the total averaged error. The average localization error  $\bar{E}$  and deviation of error  $\sigma$  are plotted. The formulae of  $\bar{E}$  and  $\sigma$  are expressed as,

$$\bar{E} = \frac{1}{L_t} \sum_{j=1}^{L_t} \left( \frac{1}{N} \sum_{i=1}^N E_i \right); \quad \sigma = \sqrt{\frac{1}{N} \sum_{i=1}^N (E_i - \bar{E})^2}, \quad (15)$$

where  $N$  is the number of AUVs in the UW-ASN,  $E_i$  represents the localization error for each AUV operating in the UW-ASN at that particular time, and  $L_t$  is the number of times the localization is performed, such that  $L_t = \frac{T_{end}}{\Delta T}$ .

### 5.1. Simulation scenarios

The parameters for our simulations are listed in Table 1.  $\alpha$  is the confidence parameter to estimate the internal and external uncertainty with  $1-\alpha$  confidence (Section 4.1). The salinity range in this table is based on typical measurements in [23]; the velocity range is based on typical underwater vehicles such as underwater gliders [23,26] and

propeller driven vehicles; and the water temperature range is based on the measurement in [25]. We further assume that ongoing communication packets are generated according to the Poisson traffic model with arrival rate being 3 packets per minute. As shown in Fig. 4, we utilize the following two specific scenarios.

**Scenario 1:** This scenario involves a team of AUVs who collaboratively explore an underwater region located under ice. These AUVs remain under-ice for the duration of the mission and do not return to the surface until the mission is completed.

**Scenario 2:** This scenario is similar to the first except that individual AUVs will periodically surface to update their positioning via GPS. These AUVs take turns to go back to the surface at a predefined interval, which is 4000 s in our simulations. Note that in practice AUVs surface every one hour [26] or every few hours [23] hence the interval selected is a reasonable value. In order to avoid ice cover, these AUVs return to the edge of the ice sheet where they were deployed. Once an AUV surfaces, it acquires a GPS fix and updates its current coordinate position (position uncertainty is also reset).

Both scenarios are tested with typical and extreme currents, whose speed ranges are listed in Table 1. A random 3D direction is chosen for the current throughout one round of simulation. The Doppler data is based on the 6-h Doppler speed measurement that we took using WHOI modems on November 20th, 2011 in the Bayfront Park bay, Lavallete, NJ, as shown in Fig. 5. Our measurement shows that most of the Doppler speeds are low, similar to the part we plot here. Note that the right hand side in (7) is replaced with the measured Doppler speed here as there is no need to calculate the Doppler shifts.

### 5.2. External-uncertainty prediction accuracy

We are interested in comparing the external-uncertainty prediction accuracy of our proposed UKF algorithm with that predicted using a simple KF. We compare the 3D sizes and probability mass functions (pmfs) between those obtained in simulations and those predicted by our model. Simulations of 100 rounds were performed for predictions of underwater gliders, and the average results are

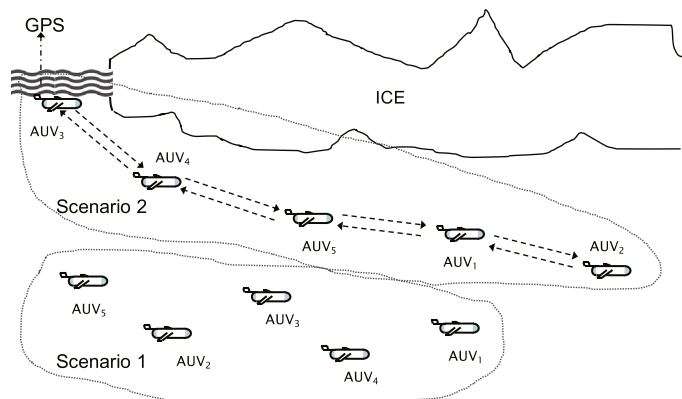
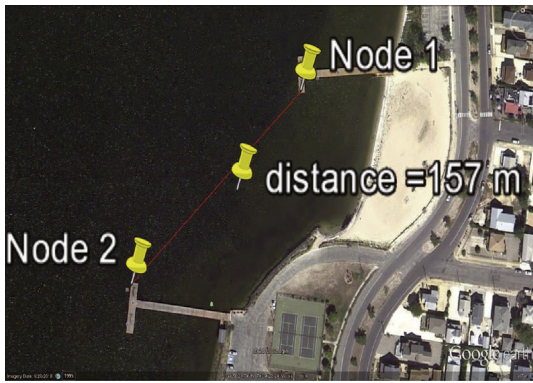
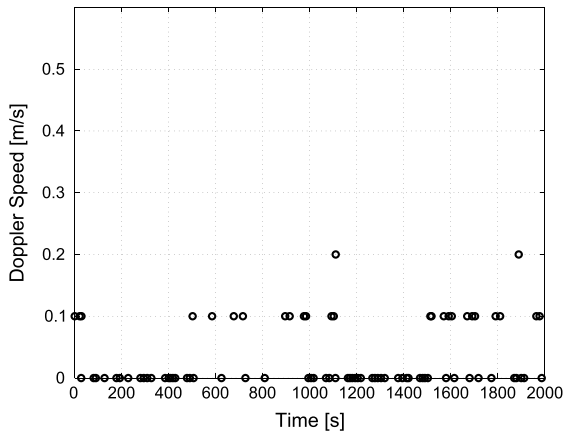


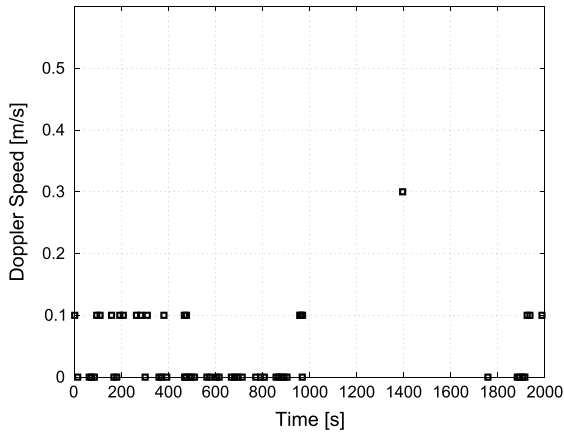
**Fig. 4.** Two scenarios for simulations: different dotted circles represent different scenarios.



(a) Location: Bayfront Park bay, Lavallette, NJ



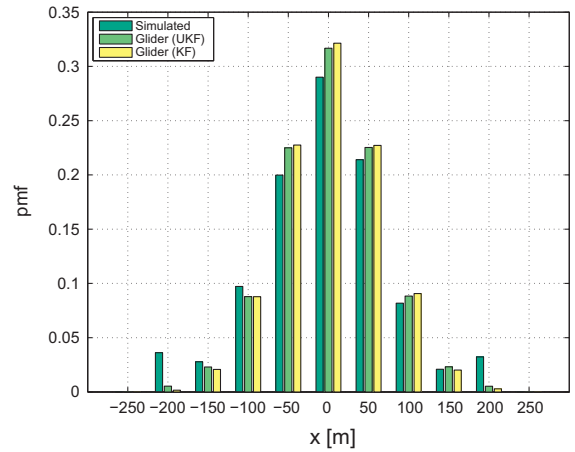
(b) Doppler speeds measured at node 1.



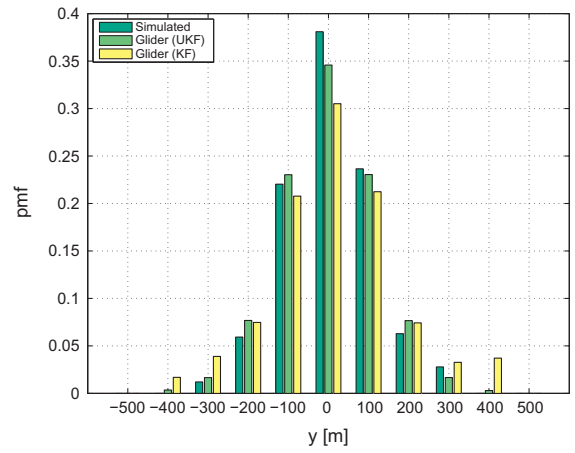
(c) Doppler speeds measured at node 2.

**Fig. 5.** Doppler speed measurement. Only part of the measurements are plotted for clear visualization. Time coordinates vary due to different reception time.

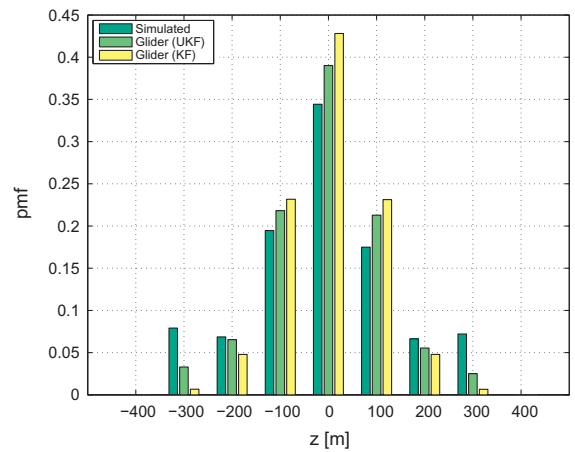
plotted in Fig. 6. Note that by ‘Glider (UKF)’ and ‘Glider (KF)’ we denote the uncertainty for a glider predicted using the UKF and KF, respectively. From these figures, we can see that our external-uncertainty model using UKF gives more accurate predictions than that using KF on the region sizes and distribution functions. In any of these axis, the



(a) pmf along the  $x$  coordinate



(b) pmf along the  $y$  coordinate



(c) pmf along the  $z$  coordinate

**Fig. 6.** External-uncertainty Prediction Accuracy: estimated 3D region probability mass functions (pmfs).

vehicle may be randomly located in a range  $[\tau - \rho/2, \tau + \rho/2]$ , where  $\tau$  is the expected location of this vehicle in this direction. We call  $\rho$  the size of the uncertainty

region as it determines the range the AUV may be distributed in. We assume that at time 0 there is no position uncertainty (e.g., AUVs are on the ocean surface where GPS is accessible) and that estimations of the external uncertainty are run at the same time. To compare the distribution functions, in Fig. 6 we also align the pmfs (i.e., move the expected positions of the vehicle in these three cases to 0). Each pmf value at a discrete position, say  $x_0$ , is calculated by checking if the vehicle lies in  $[x_0 - \psi/2, x_0 + \psi/2]$ , where  $\psi$  is the interval size. Note that the longer an AUV stays underwater, the less accurate the prediction is. Provided an accuracy threshold, our model can be used for AUVs to decide when to surface for position correction (e.g., to get a GPS fix).

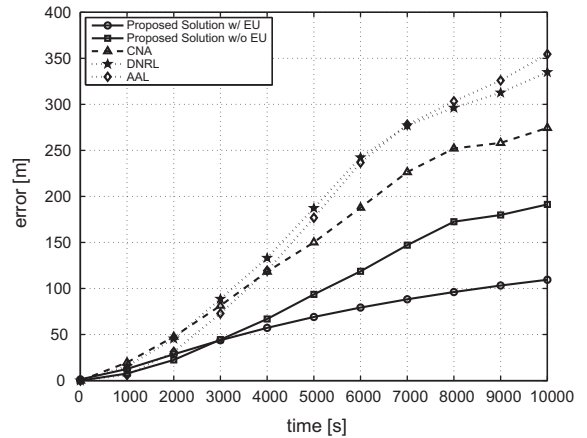
5.3. Localization performance

Real time (one simulation run) localization errors and deviations of error are plotted in the first two subfigures of Figs. 7–10. Moreover, to obtain results of statistical significance, 250 rounds were conducted for varying numbers of AUVs. The average errors for the AUV’s predicted location are plotted in Figs. 7, 8, 9 and 10(c) with 95% confidence intervals.

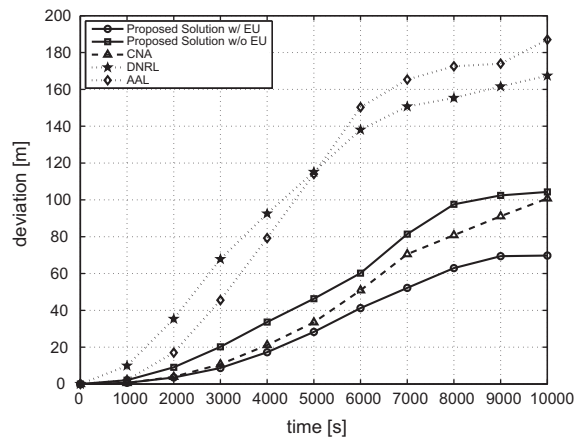
**Scenario 1:** As shown in Figs. 7 and 8, our original solution ‘Proposed solution w/ EU’ performs the best. In the typical current setting, ‘Proposed solution w/ EU’ obtains about 74.6% less error than ‘Proposed solution w/o EU’ while it obtains 80.4% less error in the extreme current setting. This is mainly due to the use of the external uncertainty model to predict the position and distribution of the AUVs and the ability to minimize the localization uncertainty. ‘Proposed solution w/o EU’ ranks the second in terms of error performance because an AUV can leverage the ongoing communications and cooperation of other AUVs for localization. Even though CNA uses EKF to predict the positions, its performance is worse than ‘Proposed solution w/o EU’ since the AUV can only use its own states for position estimation. On the other hand, CNA is still better than DNRL and AAL due to the use of EKF filter, and DNRL performs better than AAL since it takes the current influence into account.

By comparing Figs. 7 and 8, we can see that under extreme conditions, the localization error keeps increasing, since more dislocation is incurred by the extreme currents. Interestingly enough, we can see that the performance of our solution without using external uncertainty is not much better than that using CNA. In this case, using Doppler information does not help improve the localization much since the position uncertainties associated with other AUVs are also large and thus the performance is not too much better than that of using EKF. However, our solution using external uncertainty still performs the best due to the ability to estimate the position uncertainty and then use such information to minimize uncertainty.

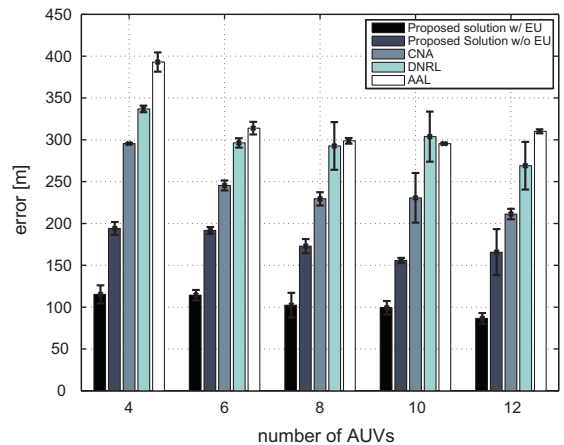
**Scenario 2:** As shown in Figs. 9 and 10, the performance ranking for these solutions closely resembles that in Scenario 1. However, the localization performance in Scenario 2 is much better than that in Scenario 1 since AUVs can obtain position correction periodically, as seen by comparing Figs. 7 with 9 (or Figs. 8 with 10). From these figures, we can see that localization error and deviation decrease when



(a) Localization error comparison (6 AUVs)



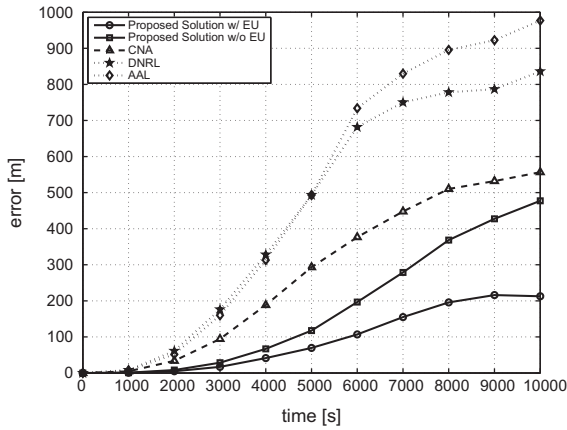
(b) Deviation comparison (6 AUVs)



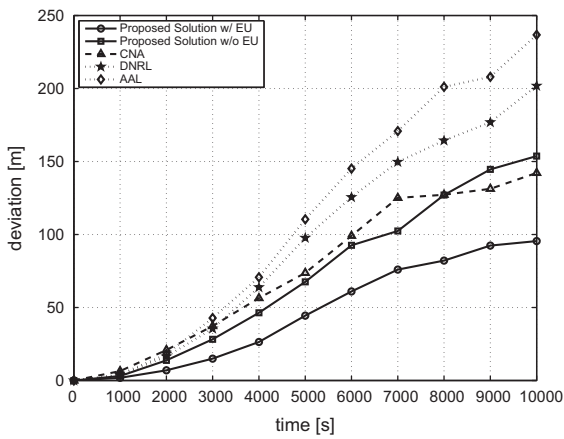
(c) Localization error for number of AUVs

Fig. 7. Scenario 1 with Typical Currents: under the ice mission with no resurfacing.

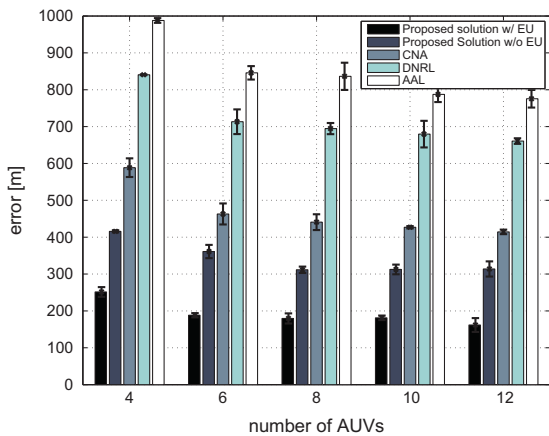
AUVs surface, i.e., at 4000 s and 8000 s in the results. Moreover, we can see that for typical current settings in Scenario 2, the localization error and its deviation can stay within certain threshold for ‘Proposed Solution w/ EU’,



(a) Localization error comparison (6 AUVs)



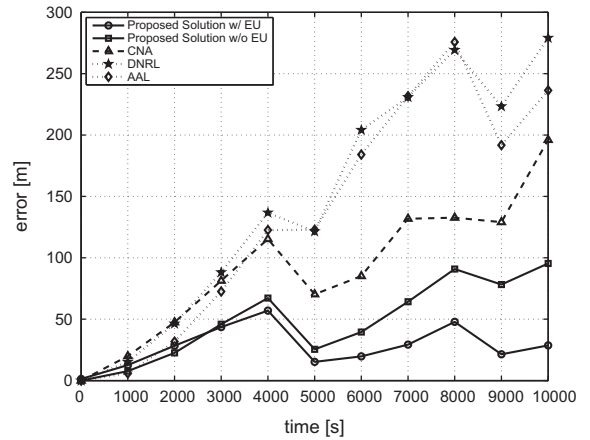
(b) Deviation comparison (6 AUVs)



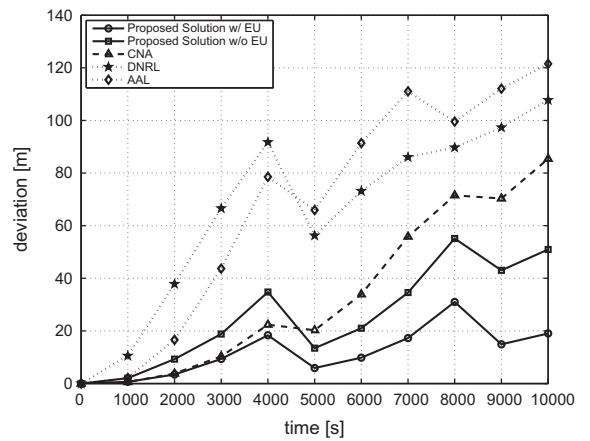
(c) Localization error for number of AUVs

**Fig. 8.** Scenario 1 with Extreme Currents: under the ice mission with no resurfacing.

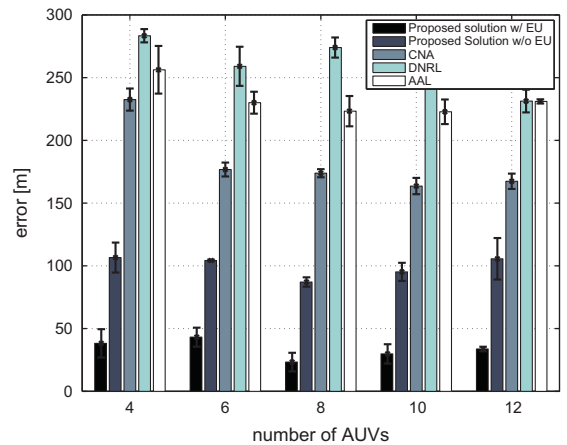
while the error of other solutions tends to increase. This shows the effectiveness of our proposed solution in minimizing the localization uncertainty.



(a) Localization error comparison (6 AUVs)



(b) Deviation comparison (6 AUVs)

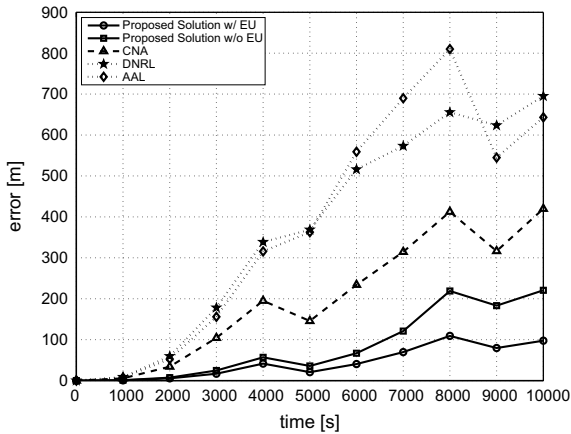


(c) Localization error for number of AUVs

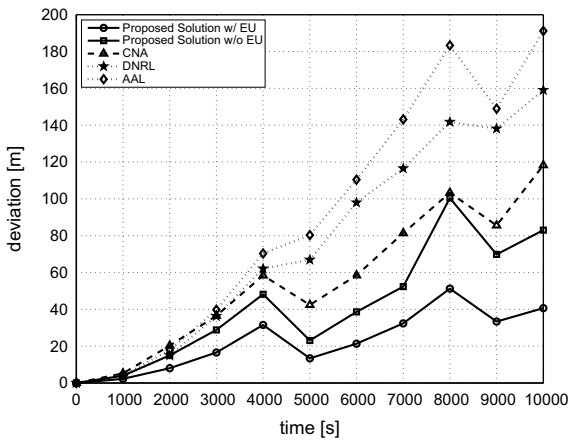
**Fig. 9.** Scenario 2 with Typical Currents: under the ice mission with resurfacing.

5.4. Communication overhead

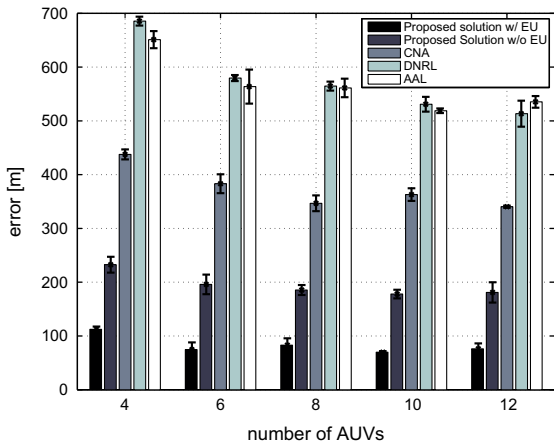
Last, we compare the communication overhead of our solutions against other solutions. As shown in Fig. 11,



(a) Localization error comparison (6 AUVs)



(b) Deviation comparison (6 AUVs)



(c) Localization error for number of AUVs

Fig. 10. Scenario 2 with Extreme Currents: under the ice mission with resurfacing.

'Proposed solution w/o EU' achieves less overhead than CNA, DNRL and AAL due to the ability to exploit the Doppler shifts of ongoing communications for localization, reducing the use of ranging packets. 'Proposed solution

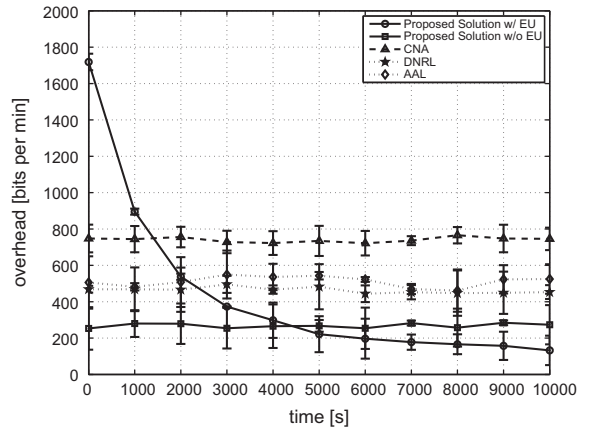


Fig. 11. Comparison of communication overhead.

w/ EU' has the biggest communication overhead in the beginning because of the need to broadcast external uncertainty information (such as pdf information). However, due to the ability to optimize the update intervals  $T_s$  and  $T_p$  as in Section 4.4, its communication overhead drops quickly to a level that is lower than CNA, DNRL and AAL. CNA has higher overhead than DNRL and AAL as CNA needs to broadcast additional information such as velocities and sensor readings for EKF while DNRL and AAL only need to broadcast the position and time information that is embedded in the ranging packet. Note that in 'Proposed solution w/ EU', to save the overhead, when the AUVs broadcast the pdf information, they only broadcast the key parameters if the pdf is one of the well-known distributions (e.g., the average and standard deviation for a normal distribution). Otherwise, the point mass function of a finite number of points is broadcast.

### 6. Conclusion and future work

We proposed a localization solution that minimizes the position uncertainty and communication overhead of AUVs in the challenging under-ice environments. With the notion of external uncertainty, position uncertainties of the AUV can be modeled in a probabilistic way. This model is further used to estimate the uncertainty resulted from localization techniques, as shown for our proposed Doppler-based localization and the standard distance-based localization. Algorithms are then proposed to minimize the position uncertainty and communication overhead. Our solution is implemented on WHOI modems and compared with several existing localization techniques using an acoustic communication emulator. It is shown that our approach achieves excellent localization results with low localization overhead. Further work will be to implement our proposed localization solution on AUV platforms and evaluate its performance in ocean experiments.

### References

[1] B. Chen, D. Pompili, Uncertainty-aware localization solution for under-ice autonomous underwater vehicles, in: Proc. of IEEE

- Conference on Sensor, Mesh and Ad Hoc Communications and Networks (SECON), Seoul, Korea, 2012.
- [2] I.F. Akyildiz, D. Pompili, T. Melodia, Underwater acoustic sensor networks: research challenges, *Ad Hoc Networks (Elsevier)* 3 (3) (2005) 257–279.
  - [3] D. Pompili, I.F. Akyildiz, A cross-layer communication solution for multimedia applications in underwater acoustic sensor networks, in: Proc. of IEEE International Conference on Mobile Ad-hoc and Sensor systems (MASS), Atlanta, GA, 2008.
  - [4] J.C. Kinsey, R.M. Eustice, L.L. Whitcomb, A survey of underwater vehicle navigation: recent advances and new challenges, in: Proc. of IFAC Conference of Manoeuvring and Control of Marine Craft, Lisbon, Portugal, 2006.
  - [5] B. Chen, D. Pompili, QUO VADIS: QoS-aware underwater optimization framework for inter-vehicle communication using acoustic directional transducers, in: Proc. of IEEE Conference on Sensor, Mesh and Ad Hoc Communications and Networks (SECON), Salt Lake City, UT, 2011.
  - [6] V. Chandrasekhar, W.K. Seah, Y.S. Choo, H.V. Ee, Localization in underwater sensor networks: survey and challenges, in: Proc. of the ACM International Workshop on Underwater Networks (WUWNet), 2006.
  - [7] M. Erol-Kantarci, L.M. Vieira, M. Gerla, AUV-Aided localization for underwater sensor networks, in: Proc. of International Conference on Wireless Algorithms, System and Applications (WASA), Chicago, IL, 2007.
  - [8] M. Erol, L.F.M. Vieira, M. Gerla, Localization with DiveN'Rise (DNR) beacons for underwater acoustic sensor networks, in: Proceedings of the ACM Workshop on Underwater Networks (WUWNet), 2007.
  - [9] M.F. Fallon, G. Papadopoulos, J.J. Leonard, N.M. Patrikalakis, Cooperative AUV navigation using a single maneuvering surface craft, *International Journal of Robotics Research* 29 (2010) 1461–1474.
  - [10] D. Mirza, C. Schurgers, Motion-aware self-localization for underwater networks, in: Proc. of ACM International Workshop on UnderWater Networks (WUWNet), San Francisco, CA, 2008.
  - [11] D. Mirza, C. Schurgers, Collaborative tracking in mobile underwater networks, in: Proc. of ACM International Workshop on UnderWater Networks (WUWNet), Berkeley, CA, 2009.
  - [12] M. Blain, S. Lemieux, R. Houde, Implementation of a ROV navigation system using acoustic/Doppler sensors and Kalman filtering, in: Proc. of IEEE International Conference on Engineering in the Ocean Environment (OCEANS), San Diego, CA, 2003.
  - [13] B. Chen, D. Pompili, Team formation and steering algorithms for underwater gliders using acoustic communication, *Computer Communications (Elsevier)* 35 (9) (2012) 1017–1028.
  - [14] I.S. Kulkarni, D. Pompili, Task allocation for networked underwater vehicles in critical missions, *IEEE Journal of Selected Areas in Communications* 28 (5) (2010) 716–727.
  - [15] P.S. Maybeck, *Stochastic Models, Estimation, and Control, vol. 1*, Academic Press, New York, 1979.
  - [16] R.V.D. Merwe, E.A. Wan, The square-root unscented Kalman filter for state and parameter-estimation, in: Proc. of International Conference on Acoustics, Speech, and Signal Processing (ICASSP), Salt Lake City, UT, 2001.
  - [17] K. Perrine, K. Nieman, K. Lent, T. Henderson, T. Brudner, B. Evans, Doppler estimation and correction for shallow underwater acoustic communications, in: Proc. of Asilomar Conference on Signals, Systems and Computers, Pacific Grove, CA, 2010.
  - [18] S. Mason, C.R. Berger, S. Zhou, P. Willett, Detection, synchronization, and doppler scale estimation with multicarrier waveforms in underwater acoustic communication, *IEEE Journal of Special Area in Communications* 26 (9) (2008) 1638–1649.
  - [19] B. Li, J. Huang, S. Zhou, K. Ball, M. Stojanovic, L. Freitag, P. Willett, MIMO-OFDM for high rate underwater acoustic communications, *IEEE Journal on Oceanic Engineering* 34 (4) (2009) 634–644.
  - [20] B. Chen, P.C. Hickey, D. Pompili, Trajectory-aware communication solution for underwater gliders using WHOI micro-modems, in: Proc. of IEEE Conference on Sensor, Mesh and Ad Hoc Communications and Networks (SECON), Boston, MA, 2010.
  - [21] W.S. Burdick, Underwater acoustic system analysis, in: A.V. Oppenheim (Ed.), *Prentice-Hall Signal Processing Series*, Prentice-Hall, 1984, p. 49 (Chapter 2).
  - [22] R.J. Urick, *Principles of Underwater Sound*, McGraw-Hill, 1983.
  - [23] O. Schofield, J. Kohut, D. Aragon, L. Creed, J. Graver, C. Haldeman, J. Kerfoot, H. Roarty, C. Jones, D. Webb, S. Glenn, Slocum gliders: robust and ready, *Journal of Field Robotics* 24 (6) (2007) 473–485.
  - [24] A. Eroshko, V. Kushnir, A. Suvorov, Mapping currents in the northern Black Sea using OLT-type profilers, in: Proc. of the IEEE Working Conference on Current Measurement, San Diego, CA, 1999.
  - [25] P.J. Stabenro, J.D. Schumacher, R.F. Davis, J.M. Napp, Under-ice observations of water column temperature, salinity and spring phytoplankton dynamics: Eastern Bering Sea shelf, *Journal of Marine Research* 56 (1) (1998) 239–255.
  - [26] C.C. Eriksen, T.J. Osse, R.D. Light, T. Wen, T.W. Lehman, P.L. Sabin, J.W. Ballard, A.M. Choid, Seaglider: a long-range autonomous underwater vehicle for Oceanographic Research, *IEEE Journal of Oceanic Engineering* 26 (4) (2001) 424–436.



**Dario Pompili** is an Assist. Prof. in the Dept. of Electrical and Computer Engineering (ECE) at Rutgers University, where he is the director of the Cyber-Physical Systems Laboratory (CPS Lab) and the site co-director of the NSF Center for Cloud and Autonomic Computing (CAC). He received a Ph.D. in ECE from the Georgia Institute of Technology (GaTech) in 2007. In 2005, he was awarded GaTech BWN-Lab Researcher of the Year. He had previously received his 'Laurea' (integrated B.S./M.S.) and Doctorate degrees in Telecommunications and Systems Engineering from the University of Rome "La Sapienza," Italy, in 2001 and 2004, respectively.

In 2011, Pompili received the NSF CAREER award to design efficient communication solutions for underwater multimedia applications and the Rutgers/ECE Outstanding Young Researcher award. In 2012, he received the ONR Young Investigator Program (YIP) award to develop an uncertainty-aware autonomic mobile computing grid framework as well as the DARPA Young Faculty Award (YFA) to enable complex real-time information processing based on compute-intensive models for operational neuroscience. He published more than 80 referred publications: with about 3000 citations, Dr. Pompili has an h-index of 20 and a i10-index of 25 (Google Scholar). He is member of the IEEE Communications Society and the ACM.



**Baozhi Chen** received his B.S. degree from Beijing University of Posts and Telecommunications, Beijing, China, in 2000. He received his M.S. degree from Columbia University in New York City in 2003. In 2012, he received his Ph.D. degree in Electrical and Computer Engineering at Rutgers, the State University of New Jersey – New Brunswick, under the supervision of Prof. D. Pompili. His research interests lie in underwater communications and networking, communication and coordination of autonomous underwater vehicles,

and wireless communications and networking, wireless sensor networks, and wireless body-area networks. He was a co-chair of work-in-progress poster session in ACM WUWNet'12. He also served as technical program committee member in BodyNets'10, GreenNets'11, and GreenNets'12, and as reviewer for ACM and IEEE journals and conferences.